María José Legaz
C. Guedes Soares
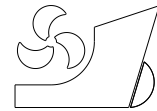
EVALUATION OF VARIOUS WAVE ENERGY CONVERTERS IN THE BAY OF CÁDIZ

Summary

The Andalusian Agency of Energy has identified three areas of major interest for harnessing wave energy, in their plan of "Marine Energy and Energy Resources of Andalusia". One of these areas is located on the Atlantic coast, the bay of Cádiz. Considering this initial interest, the objective of this work is to carry out an evaluation of the performance provided by various technologies of wave energy conversion in the bay of Cádiz. The data for the wave climate in the target area are obtained from the Spanish Agency Puertos del Estado. Diagrams for bivariate distributions of the sea states occurrences, defined by the significant wave height and the energy period, are shown. On this basis, the output of nine different technologies for the conversion of wave energy is assessed in the reference locations in the bay of Cádiz. According to the results obtained, it can be said that the bay of Cádiz is a suitable place for wave energy extraction.

Key words: Bay of Cádiz; wave energy; WEC

1. Introduction

Nowadays, there is a general concern about global warming. Several energy trans-formations are being studied and tested: solar, wind and marine energy. It seems that marine energy and more specifically wave energy has a high energy density and good predictability. For these reasons, it is stated that wave energy has great potential and a promising future.

The previous attributes make wave energy a good candidate for its utilization as a source of renewable energy. To characterize the ocean wave energy, numerical modelling is one of the most used methods. Guedes Soares et al. [1] has studied various coasts in Europe including the Iberian Peninsula, which was studied in more detail by Silva et al. [2, 3]. Studies have also been made in islands, Rusu et al. [4], where a wave prediction system based on WAM and SWAN spectral phase averaging wave models were implemented and tested for Madeira Archipelago. Iglesias and Carballo [5] used the WAM model to assess the wave resource in El Hierro. Rusu and Guedes Soares [6] assessed the wave energy in the Azores Islands in a first step considering remotely sensed and historical data and in a further step based on spectral models. Sierra et al. [7], wave energy re-sources in Lanzarote, is analysed using series of data. Gonçalves et al. [8], the WAVEWATCH III model is used to generate

waves for the entire North Atlantic basin and the SWAN model is used to determine the transformation of the waves in the Canary Islands. Ponce de León et al., [9] study the wave energy availability in Balearic Sea implementing WAM model and Bernardino et al. [10] used the SWAN model to evaluate the wave energy resources in the Cape Verde Islands.

It is worth mentioning that these models can also be used to study the combined effects of waves and tides using the SWAN model as was done for the coast of Peniche [11] as well as the effect of the wave devices on the wave fields located at the north of Peniche, and in Aguçadora [12, 13].

A study about the estimation of the wave energy potential in Sicily (Italy) was carried out using both buoy wave measurements from Rete Ondametrica Nazionale (RON), the Italian Government wave buoy network, and wave parameter data by ERA-INTERIM, a recent meteorological reanalysis project of the European Centre for Medium-Range Weather Forecasts (ECMWF) can be found in [14]. An assessment of the offshore wave energy potential in the Croatian part of the Adriatic Sea is performed using data taken from World Waves atlas (WWA). WWA is based on satellite measurements, validated against buoy measurements and reanalysed by numerical wave modelling can be seen in [15]. The wave energy resource along the Northern Spanish coast is determined, on hindcast results of WAVEWATCH III for the Atlantic Ocean area, coupled with the SWAN model for the coastal areas, and using surface winds from ECMWF's ERA- Interim data base can be found in [16].

To estimate the energy produced by a wave energy converter (WEC) system in a certain period of time, the most common method is to associate the power matrix of the WEC system to the environmental matrix from the considered area in the determined time interval. This process can be used to evaluate the optimum location of a WEC, but also to identify the most efficient WEC for a given area. After having the wave energy conditions at a given location the performance of different types of wave energy devices have been studied for the Portuguese nearshore [17].

The Andalusian Energy Agency has carried out a study named "Marine Energy and Energy Resources of Andalusia" [18], providing the estimated the harvesting possibilities of clean energy from seas and oceans of the Andalusian Autonomous Community. This report has identified the bay of Cádiz as an interesting area to obtain wave energy.

Based on this fact the objective of this paper is twofold. On the one hand, studying what would be the most appropriate location to install the wave energy converters (WECs) in the bay of Cádiz. On the other hand, studying what is expected from different types of WECs at the different reference locations.

This paper is structured as follows. Section 2, a brief description of the characteristic of the bay of Cádiz and selection of the reference locations is made. Data and parameters of the wave-field in the bay of Cádiz and the scatter diagrams of the reference locations are given in section 3. Section 4 presents the results of the electric power of the different WECs in the reference locations. Section 5, a discussion of the results is made. In section 6, the conclusions are highlighted.

2. Target area

The area of interest is the bay of Cádiz. This area has been identified by the Andalusian energy agency as one of the zones with high potential to obtain wave energy, see the report on marine energies, energy resources of Andalusia (Phase I) [18].

The bay of Cádiz is located in the province of Cádiz, Andalusia, southwestern in Spain. The coordinates of the province of Cádiz are *36° 31' 37.42'' N, 6° 17' 18.95'' W*. The province of Cádiz has a population of *1.239.435*, according to the Spanish statistical office 2017 [19]. On the other hand, the bay of Cádiz has a high per capita energy consumption compared to the rest of Andalusia, according to the Andalusian energy agency. The primary energy consumption in 2015 was *4.687,7* KTep (Kilo-Ton equivalent of petroleum). Figure 1 shows the location of the Bay of Cádiz with a big red dot
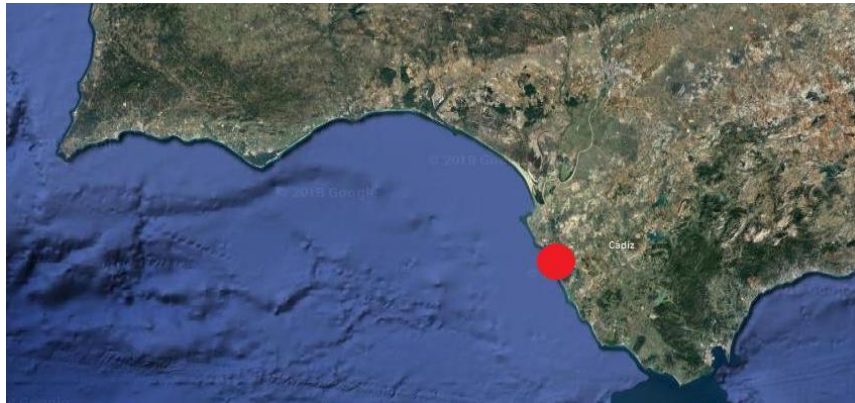

Fig. 1 Bay of Cádiz. Southwestern of Spain.

2.1   Reference locations

A wave energy installation could be proposed to meet the energy demand in the bay of Cádiz. Since the wave resource changes with water depth and other characteristics due to the different processes that affect the wavefield during propagation, it is necessary to consider several reference locations. In the environment of the bay of Cádiz has been selected as reference points the two buoy of Cádiz and the SIMAR points that are in line with these buoys.

The reference points are divided in two groups: onshore and offshore points, figures 2 and 3. The offshore points are the Cádiz buoy, and the SIMAR points 5032015, 5034015 and 1054046 and 5026015 shown in table 1. The coastal points are the Cádiz coastal buoy and the SIMAR 6008050 point, see table 2.

Fig. 2 The buoy of Cádiz and Coastal buoy of Cádiz. Source: Puertos del Estado.

Fig. 3 SIMAR points: 5026015, 5032015, 5034015, 1054046, 6008050. Source: Puertos del Estado.

Table 1 Longitude, latitude, and depth of the Cádiz buoy and the SIMAR offshore points (WAM model). Source: Puertos del Estado.

OFFSHORE POINTS	LONGITUDE	LATITUDE
CÁDIZ BUOY	-6.963 E	36.477 N
SIMAR 5032015	-6.833 E	36.500 N
SIMAR 5034015	-6.667 E	36.500 N
SIMAR 1054046	-6.500 E	36.500 N
SIMAR 5026015	-7.333 E	36.500 N

Table 2 Longitude, latitude, and depth of the Cádiz coastal buoy and the SIMAR nearshore (WAM model). Source: Puertos del Estado.

NEARSHORE POINTS	LONGITUDE	LATITUDE
COASTAL CÁDIZ BUOY	-6.330 E	36.500 N
SIMAR 6008050	-6.367 E	36.583 N

3. Material and methods

3.1 Data and parameters of the wave-field in the bay of Cádiz

The Spanish Puertos del Estado [20], is a state company in charge of the management of the Spanish state ports. This company carries out the Government's port policy and co-ordinates and controls the efficiency of the port system, which consists of 28 port authorities that manage the 46 ports of general interest. Puertos del Estado has a web page showing the

weather forecast in real-time. On the website, there are predictions, real-time data and historical data of waves, wind, currents, salinity and seawater temperature.

To provide reliable information, Puertos del Estado has several buoys located around the Spanish coastline and use mathematical models to obtain information about the waves. From the website of Puertos del Estado, the diagrams Hs(m) and Tp(s) for the reference locations have been obtained. These diagrams are used to assess the energy of the waves in the Bay of Cádiz.

Data from different SIMAR points both on the offshore and near the coast are obtained from the website of the Puertos del Estado. The SIMAR data set consists of the time series of wind and wave parameters obtained by numerical modelling. Therefore, they are synthetic data and do not come from direct measures of nature. The SIMAR series arises from the concatenation of the two large groups of numerically modelled wave data that the Puertos del Estado has traditionally counted: SIMAR-44 and WANA. The objective is to be able to offer longer time series in the time interval and updated daily. In this way, the SIMAR set offers information from 1958 until today.

3.1.1   Cádiz buoys

In the bay of Cádiz, there are two buoys belong to Puertos del Estado an offshore buoy named Cádiz buoy and an onshore buoy named coastal buoy of Cádiz.

The Cádiz buoy is a SeaWatch [21] type buoy that consists of a stable platform where several instruments can be placed to measure and monitor the marine environment in real time. The buoy is composed of a central part of lenticular form, which provides buoyancy and houses the computer and several electronic equipment, and three masses or vertical supports *6* meters long, located in such a way that half of its length is above the water (providing support for meteorological sensors) and the other half below (housing of oceanographic sensors). The batteries that provide power to the assembly work with solar panel energy. The total length of the buoy (including the sensors) is approximately *6.5* m, its diameter of *1.8* m and its approximate weight of *600* Kg, as in figure 4, on the left. The basic quality control that has been established for all parameters consists in rejecting those that exceed a maximum value and those that present differences with adjacent data greater than a certain threshold. The specific values mentioned have been determined by the experience of each station and parameter. This simple quality control cleans the vast majority of spurious data but does not prevent some abnormal data from being considered correct, so it is convenient to subsequently make a final correction "by hand".

The coastal buoy of Cádiz is a Triaxys type buoy [22] that has a spherical shape of *91* cm in diameter. It has a water temperature sensor, solid-state accelerometers, a piezo gyroscope and a microprocessor-controlled compass, as in figure 4 on the right. Data processing is carried out on board the buoy using the six motion sensors and the compass. The data analysis is based on the numerical solution of the nonlinear equations of the buoy movement with respect to a fixed reference system. The signal is transmitted by radio to a digital receiver on land, where the various scalar parameters (spectral and zero-crossing) and directional parameters that characterise the sea states are stored in real-time. The wave variables are the result obtained from the application, to the time series of instantaneous elevations, of rigorous quality control prior to the statistical (short term) and spectral (FFT) analysis. The quality control performs verifications aimed at detecting specific errors in the series (peaks, atypical accelerations, anomalous periods, etc.) and of anomalous global behaviours (bias, kurtosis, etc.). The most representative parameters obtained from the analyses are subject to several consistency criteria to try to detect the possible anomalous operation of the measuring equipment. Finally, the results are validated by verifying them by

Fig. 4 On the left buoy of Cádiz, on the right coastal buoy of Cádiz. Source: Puertos del Estado.

comparison with other available sources of data as well as by the results of the calibration of the buoy made, after its recovery, in the laboratory.

3.1.2   Subset SIMAR-44

The SIMAR-44 set results from a high-resolution analysis of the atmosphere, sea level, and waves that cover the entire Spanish coastal environment. Puertos del Estado simulated the atmosphere and waves in the Mediterranean basin within the framework of the European project HIPOCAS [23]. The wave data in the Atlantic domain and the Strait of Gibraltar come from two independent wind and wave simulations, one conducted by the Puertos del Estado and the other conducted by the Mediterranean Institute for Advanced Studies (IMEDEA) within the framework of the VANIMEDAT-II project. Below is a brief description of how each of the simulated agents was generated.

Mediterranean wind data has been obtained using the REMO regional atmospheric model forced by the data from the NCEP global reanalysis. That reanalysis assimilates ins-trumental and satellite data. The REMO model has been integrated using a *30′* longitude by *30′* latitude mesh (approximately *50* km by *50* km) with a *5* min time step. The wind data provided are averages per hour at the height of *10* m above sea level. To obtain wind data in the Atlantic and the Strait of Gibraltar, the RCA *3.5* model is used. This model is fed with reanalysis data obtained from global atmospheric ERA-40. These simulations were performed by the Meteorological Statal Agency [24] with a mesh resolution of *12′* latitude by *12′* longitude (approximately *20* km by *20* km). Due to the resolution of the meshes used in REMO and RCA *3.5* models, it is not possible to model neither the effect of orographic accidents of less than *50* km nor the influence on the wind of local convective processes modelled. However, the model correctly reproduces regional winds induced by topography such as Cierzo, Tramontana and Mistral. In general, the reproduction of situations with winds from the sea will be more reliable.

To generate the wave fields, the WAM numerical model has been used. This applica-tion is a third-generation spectral model that solves the energy balance equation without establishing any prior hypothesis about the shape of the wave spectrum. The data has been

generated with an hourly rate. A decomposition of the sea of wind and swell has been made. In order to describe situations with swell crossed seas, the possibility of two swell contributions has been considered. For the Mediterranean area, a variable spacing mesh has been used with a resolution of *15′* of latitude x *15′* of longitude (approximately *25* km x *25* km) for the east edge of the mesh and *7.5′* of latitude x *7.5′* of longitude (approximately *12.5* km x *12.5* km) for the rest of the modelled area.

On the other hand, a variable spacing mesh covering the entire North Atlantic has been used for the Atlantic area with a resolution of *30′* latitude x *30′* longitude for the areas furthest from the Iberian Peninsula, and the Canary Islands increases to *15′* latitude x *15′* longitude when approaching. For the surroundings of the Gulf of Cadiz, the Strait of Gibraltar and the Canary Islands, secondary meshes have been nested to the main mesh with a resolution that reaches *5′* longitude x *5′* latitude. The WAM model used to generate this data includes refraction and wave shoaling effects. However, given the resolution of the model, the wave shoaling effects can be considered negligible. Therefore, for practical use, wave data should always be interpreted as data in open water at infinite depths.

3.1.3   Subset WANA

The WANA series come from the sea state prediction system that Puertos del Estado [20] has developed in collaboration with the Meteorological Statal Agency (AEMET) [24]. However, WANA data is not prediction data, but diagnostic or analysis data. This means that for each moment, the model provides wind and pressure fields consistent with the previous evolution of the modelled parameters and consistent with the observations made. It is important to note that the wind and wave time series of the WANA set is not homogeneous since wind and wave models are periodically modified to introduce improvements. These improvements have allowed, among other things, to increase the spatial and temporal resolution of the data from which the WANA set information is generated. Below is a brief description of how each of the simulated agents was generated.

The atmospheric model used to generate the wind fields is the HIRLAM (High Resolution Limited Area Model) [25], from AEMET [24]. This is a mesoscale and hydrostatic atmospheric model. The wind data provided is *10* meters high above sea level. The wind data do not reproduce geographic effects or temporal processes of scales lower than the resolution with which the atmosphere model has been integrated. However, the model correctly reproduces the regional winds induced by topography such as Cierzo, Tramontana and Mistral.

To generate the wave fields, two models have been used: WAM and WaveWatch, fed by the wind fields of the HIRLAM model. Both are third-generation spectral models that solve the energy balance equation without establishing any a priori hypothesis about the shape of the wave spectrum. The spatial resolution of the models varies depending on the area since specific applications have been developed for different areas: Atlantic, Mediterranean, Cantabrian, Cadiz, Canary Islands and Strait of Gibraltar. A decomposition of wind and swell has been carried out. In order to describe situations with crossed swells, two possible contributions to the swell have been considered. It is important to keep in mind that, regardless of the coordinate assigned to a WANA node, wave data should always be considered as data in open water and indefinite depths.

WAM wave generation model integrates the basic transport equation. This equation describes the evolution of a two-dimensional ocean wave spectrum without additional assumptions regarding the spectral shape.

The model was developed by a broad number of researchers from different institutions (WAMDI group), following 'Sea Wave Modeling Project' recommendations. One of the aims

of the group was to develop an operational version of the model at the European Centre for Medium Range Weather Forecasts (ECMWF). This was achieved in 1992. In 1996 Puertos del Estado joined the group and has collaborated in different aspects of the work done. The group final report was released in 1994. Puertos del Estado developed and implemented a two-way nesting procedure in the model for the Spanish Coast.

Using this system, the equation is integrated in the same time step for all points. Since it is possible to define the spacing depending on the grid point location, it works as a variable spacing schema. The resolution is enhanced using intermediate grids, which are placed between the coarse and the fine grids. The version of the WAM model, the distribution of grids has changed. The deep water WAM model is run for the Atlantic-Mediterranean domains, therefore the shallow water effects are not performed. Nested to this domains, specific applications have been developed for the Peninsula, Canary and Balearic Islands domains. All these latter applications use the shallow water version of the WAM model; therefore, refraction and attenuation effects are considered for those (few) grind points located in swallow waters.

The regional scale grid (Atlantic-Mediterranean) use ECMWF HRES model wind forcings, whereas the rest of the applications, given that they are within the AEMET HARMONIE spatial coverage, are forced with this model. Since HARMONIE model forecast length is 48 hours, HRES model is used for the last hours to extend this length until *72* h.

The model produces the wave directional spectra for each grid point. Then, it is used to obtain further information, i.e.: Hs, Tp, Tm, mean direction, wind sea and swell components, etc.

The WAVEWATCH model solves the wave action balance equation in the presence of currents.

The nested WAVEWATCH application covers the Strait of Gibraltar with a resolution of 1 min and receives boundary conditions from both, the Mediterranean and the Atlantic applications.

With this scheme, combining the two-way nesting procedure with local nested grids, the Spanish coast is covered with at least a resolution of *5* min with the ocean system. This resolution is further increased by the local system in which the different local applications have a resolution between *200* and *500* m. The ocean wave forecast system is operated on a twice a day cycle, and the results, maps, time series and tables can be looked up at the Spanish Meteorological Service web page, www.inm.es, which is open and free for all users. The forecast results are verified on real time using the data from Puertos del Estado buoy network. The results from this real time verification process are shown at the same web page, so the users are able to get a hold of both, the forecast itself as well as the accuracy of the previous days forecast cycles.

3.1.4   Scatter diagrams of the reference locations

Scatter diagrams are summarizing the wave climate and are typically representing the joint probability of wave height, wave period combinations during the period they are encompassing. Figures 5 and 6 show the scatter diagram, the joint distribution of significant wave height (Hs) and the peak period (Tp), in %, for the reference locations. Data have been obtained from the website of Puertos del Estado for the buoy of Cádiz, coastal buoy of Cádiz and different SIMAR points. Each bin of the graph represents the joint probability, in %, of a specific state Hs-Tp. Hs (significant height) bins are defined in *0.5* m. intervals were ranging from *0* to *6* meters. Tp (peak period) bins are defined in *1.0* s. intervals were ranging from *0*

to *11* seconds. The colour of each bin represents the number of occurrences expressed in percentage of all observations.

For the Cadiz buoy, the highest value of the joint distribution, superior to *8*% is obtained for Tp=*5*s and Hs=*1*m (Fig. 5). For 5026015 SIMAR point, the highest value of the joint distribution, about 11% is obtained for Tp=*11*s and Hs=*1.5* m (Fig. 5). For 1054046 SIMAR point, the highest value of the joint distribution, about 11% is obtained for Tp=5s and Hs=*1*m (Fig. 5). For 5032015 SIMAR point, the highest value of the joint distribution, about *11*% is obtained for Tp=*5*s and Hs=*1.5* m (Fig. 5). For 5034015 SIMAR point, the highest value of the joint distribution, about *11*% is obtained for Tp=*11*s and Hs=*1.3* m (Fig. 5).

The period of study has been five-year time interval January 2010-December 2014. The significant height, Hs, is one of the most widely used parameters of waves, represents the height of waves that a trained observer would determine with the naked eye from an observation position. It is accepted to be equivalent to the mean value of the *1/3*rd highest waves recorded in the measuring interval. The mean period, Tm, describes the mean value of the period from the waves recorded in the measuring interval. The peak period, Tp, is the period of the most energetic group of waves. The more regular are waves, the more Tp and Tm look alike, though usually, Tp is bigger than Tm. The power matrix of a WEC is given in function of the peak period Tp, or mean period Te.

In general, the instrumentation does not provide the wave features with the form of Te. It can be estimated based on Tp as [25]:

$$Te = \alpha Tp, \tag{1}$$

The coefficient α depends on the shape of the wave spectrum. In assessing the wave energy resource in southern New England, Hageman [26], assumed that $Te = Tp$. In this study, the same assumption was adopted when necessary.

3.2   Wave energy conversion technologies

From the point of view of wave energy, the energy is divided into two groups, potential and kinetic energy components [27]. Over the years, the WECs designers have had tried to transform the wave energies into electrical energy. The first patented WEC was registered in 1799 in France. Since then, until now, more than *1000* devices have been patented with different mechanisms to transform wave energy in electric energy [28]. The WECs can be classified according to water depth and location of application, type, and size of the considered WEC and working principle in which wave energy can be absorbed [29].

According to location, the WECs can be classified as shoreline, near-shore and deep-water offshore. Shoreline WECs are placed near to the utility network. This location has the disadvantage of the wave are attenuated as they travel through shallow water, so their energy decreases. Nearshore devices are put in shallow water; the disadvantage also is the reduction of wave power, limiting the harvesting potential. Offshore WECs are placed in deep water.

Considering type and size [30, 29], the devices can be categorized as line absorbers and point absorbers. The line absorbers are those in which their horizontal direction is comparable or larger than typical wavelengths; these can be attenuator or terminator. The attenuator is the one in which the larger horizontal dimension of the WEC is parallel to the wave propagation direction. The terminator is the one in which the wave propagation is normal compared to the longer horizontal direction of the WEC. Point absorbers WECs are those in which horizontal dimensions are small compared to the wavelength of the incident waves.

Within the categories identified above, there is a further level of classification of devices, determined by their mode of operation. For this work, several WECs have been selected. This WECs belong to different categories and are representative of a variety of sizes and working principles. These WECs are Wave Dragon, Pelamis, Aqua Buoy, Archimedes Wave Swing, Langlee, Oceantec, OE Buoy, Pontoon, Seabased AB, Wavebob and SSG.

Wave Dragon is an overtopping WEC. This WEC gets the wave by mean a pair of large curved reflectors, the wave is gathered into the central receiving part. From this central part, the waves flow up a ramp and over the top into a raised reservoir. The water re-turns to the sea through several low-head turbines.

Pelamis is an attenuator WEC. It is a floating device form of cylindrical hollow steel segments connected to each other by two degrees of freedom hinged joints. Each hinged joint is like a universal joint. The central unit of each joint has a system of power conversion. The cylinders operate like pumps; they drive fluid through a hydraulic motor. These hydraulic motor drives an electrical generator.

Aqua Buoy is a point absorber WEC. It is formed by a floater, providing buoyancy to the system. The floater is joined to a large cylinder, called the accelerator tube. The accelerator tube is opened to ingress water on both sides. The accelerator tube has a piston in the center, and this is joined to the top and the bottom section of the buoy by a hose pump, which is made of semi-elastic material. The system is designed in such a way that the natural that the natural frequencies of the piston and the buoy are different, resulting in significant relative motions between the two. This stretch or compress the hose pump. The water in the pump is driving by a system of check valves, through a hydraulic system that terminates into a Pelton turbine. This turbine is that it generates electricity.

AWS (Archimedes Wave Swing) is a point absorber WEC. AWS is totally submerged. This device uses the pressure difference between wave crests and troughs. It consists of a sea bed fixed air-filled cylindrical chamber with a moveable upper cylinder. When a crest goes over the WEC, the water pressure above the device compresses the air within the cylinder, moving the upper cylinder down. When a trough goes over, the water pressure on the device reduces, and the upper cylinder rises. When a crest goes over the WEC, the water pressure above the device compresses the air within the cylinder, moving the upper cylinder down. When a trough goes over, the water pressure on the device reduces, and the upper cylinder rises.

Langlee is an oscillating wave surge converter. Its function is to extract the kinetic energy of the water particles of the waves. This is achieved by a number of hinged flaps located under the water surface. It consists of a pair of working flaps that are placed symmetrically opposing each other; both installed on a moored floating frame (a semi-submerged steel structure).

Oceantec is a point absorber WEC. Its working principle is based on the oscillating water column. It is formed of interacting bodies, so that energy is extracted from its relative movement. This system requires the existence of bearing and guidance elements to guide the movement of one body along with another.

OE Buoy is a water column WEC. This consists of a single air chamber and is free to move in six degrees of freedom. The water column has a submerged opening aligned downstream of the incident wave propagation direction. An oscillating pressure in the chamber and airflow through the turbine is generated by the motion of the water column relative to the oscillating water column body. The system also has a relief valve in order to keep the pressure in the air chamber within acceptable limits. The power conversion is provided by means of an air turbine connected to an electric generator.

Pontoon is a multibody floating WEC. It consists of many heaving buoys jointed to a submerged reference structure. This structure consists of an arrangement of a single sup-port structure and a series of ballasts baskets, jointed by tension wires. A balance of forces is made by the total buoyancy forces form the buoys and the net gravity forces of the bridge and the ballast baskets. This system uses a hydraulic power take-off system to convert energy.
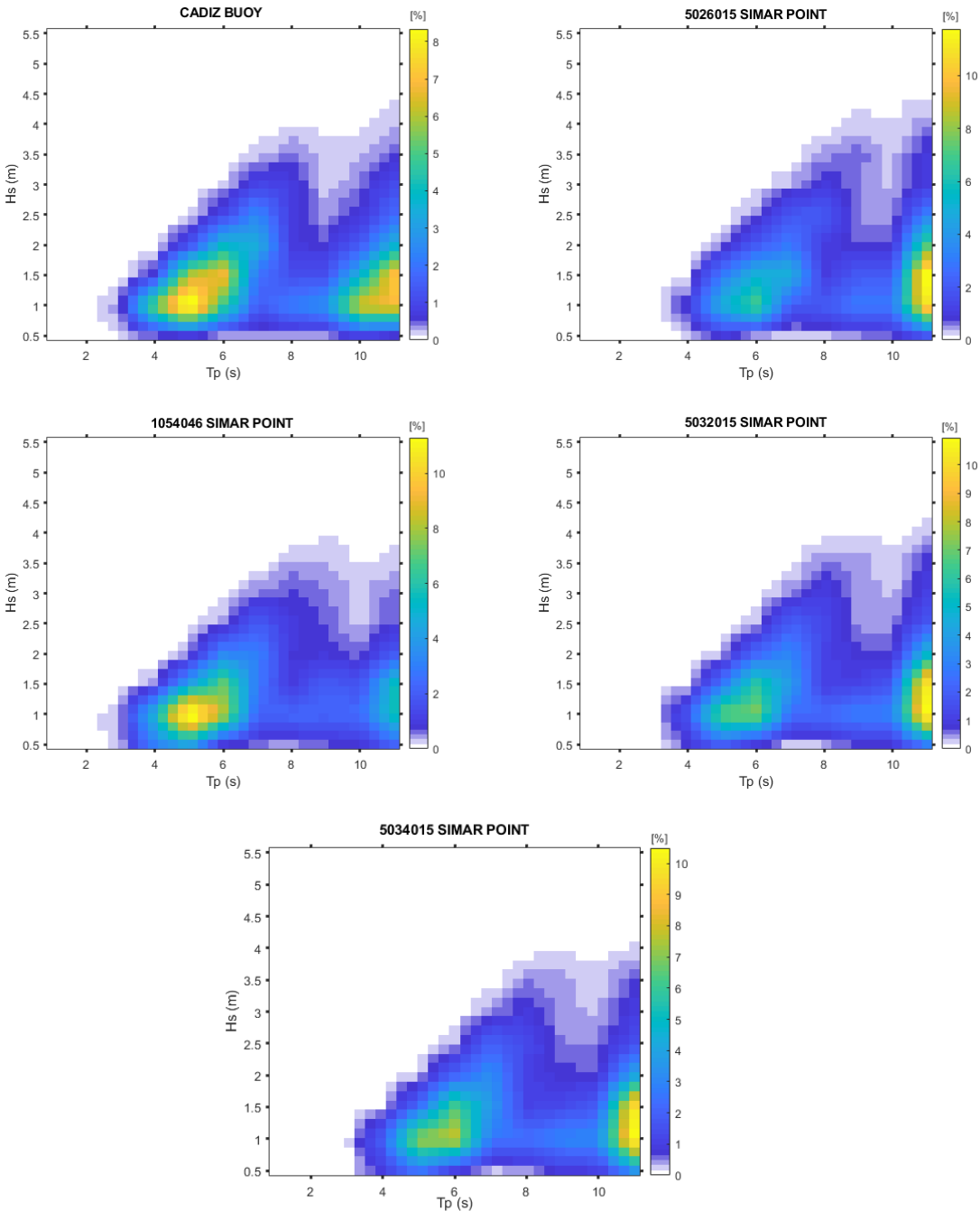

Fig. 5 On the left scatter diagram of buoy of Cádiz and 1054046 SIMAR point for the five-year time interval 2010 to 2014. On the right scatter diagram of 5026015, 5032015 SIMAR points for the five-year time interval 2010 to 2014. In the middle, scatter diagram of 5034015 SIMAR point for the five-year time interval 2010 to 2014. Source: Adapted from Puertos del Estado.
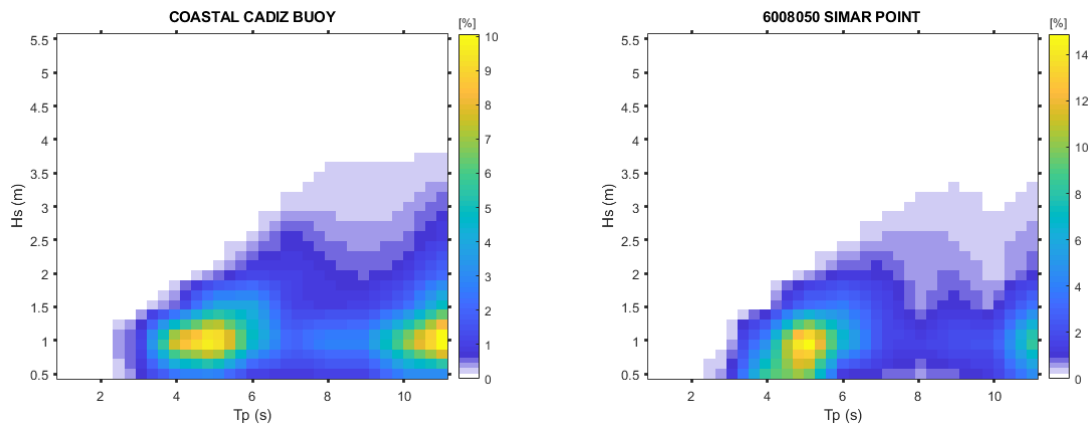
Fig. 6 On the left scatter diagram of coastal buoy of Cádiz for the five-year time interval 2010 to 2014. On the right scatter diagram of 6008050 SIMAR point for the five-year time interval 2010 to 2014. Source: Adapted from Puertos del Estado.

Oyster is formed by a system that comprises a buoyant flap, hinged at its base to a sub-frame which is pinned to the sea bed using tensioned anchors. The surge component in the waves forces the flap to oscillate which in turn compresses and extends two hydraulic cylinders mounted between the flap and the sub-frame which pumps water at high pressure through a pipeline back to the beach.

Wavebob is classified as a point absorber WEC. This device utilizes the lift and fall of the ocean wave to move the generators. It is formed by two oscillating structures. These structures are directed by a damping system that can respond to predicted wave height, wave power, and frequency. It has a semi-submerged body, the tank structure, which uses captured seawater mass as its inertial mass.

The SSG (Sea Slot-cone Generator) is a wave energy converter of the overtopping type. The structure consists of a number of reservoirs one on the top of each other above the mean water level in which the water of incoming waves is stored temporarily. In each reservoir, expressively designed low head hydro turbine is converting the potential energy of the stored water into power. The key to success for the SSG will be the low cost of the structure and its robustness.

The power matrix of the different system of WECs can be found in different research works, such as [31] and [32]. In the appendix the tables of the power matrix of the different WECs are shown.

4. Results

The most appropriate WECs for a specific area are those that have maximum efficiency in the ranges of Hs and Te, that provide the bulk of occurrences of the waves. The performance of a WECs is provided in tables showing the expected power output (power matrix) for the different pairs of significant wave height and wave period.

To estimate the energy produced by a WEC system in a certain period of time, the most common method is to associate the power matrix of the WEC system to the environment matrix (scatter diagram) of a reference location in the determined time interval. This can be done using the equation.

$$P_E = \frac{1}{100} \cdot \sum \sum p_{ij} \cdot P_{ij},$$
(2)

where p_{ij} is the energy percentage corresponding to the cell defined by line i and the column j in the environmental matrix (scatter diagram), while P_{ij} is the electric power reported by the WEC system (power matrix) in the same cell.

Table 3, represents the average electric energy production in kW of different types of WECs: Pelamis, Aqua Buoy, AWS, Langlee, Oceantec, Pontoon, OE Buoy, Wavebob and Wave Dragon in the different offshore reference localizations: Cádiz buoy and SIMAR points 5032015, 5034015,1054046 and 5026015.

Table 4 represents the average electric energy production in kW of different types of WECs: AWS, Langlee, Oceantec, Oyster, OE Buoy, Wavebob, Wave Dragon and SSG, in the different nearshore reference localizations: Cádiz coastal buoy and SIMAR point 6008050.

Table 3. Average electric power in kW for five offshore reference points in the bay of Cádiz, estimations corresponding to the characteristics of nine WEC devices.

Average Electric Power (in kW)					
POINTS					
WECs	CÁDIZ BUOY	SIMAR 5032015	SIMAR 5034015	SIMAR 1054046	SIMAR 5026015
PELAMIS	73.9	74.5	69.8	61.3	84.2
AQUA BUOY	22.0	37.9	21.9	17.7	28.2
AWS	124.7	140.6	128.9	110.5	171.7
LANGLEE	80.0	75.9	72.3	70.1	81.1
OCEANTEC	110.8	109.3	105.0	101.1	115.2
PONTOON	202.2	198.4	188.5	182.6	216.9
OE BUOY	111.6	117.2	108.8	92.1	136.6
WAVEBOB	78.5	83.1	77.1	62.0	98.1
WAVEDRAGON	342.1	1143.6	1043.5	837.3	1328.7

Regarding offshore devices, it can be observed (table 3) that for the converters Pelamis, AWS, Langlee, Oceantec, Pontoon, OE Buoy, Wavebob and Wave Dragon the optimal energetic distribution occurs in location 5026015 SIMAR point. The electric power expected in this location is *84.2* kW for Pelamis, *171.1* kW for AWS, *81.1* kW for Langlee, *115.2* kW for Oceantec, *216.9* kW for Pontoon, *136.6* kW for OE Buoy, *98.1* kW for Wavebob and *1328.7* kW for Wave Dragon.

Passing now to the nearshore devices (table 4), it can be observed that for the converters considered, the optimal energetic distribution occurs in location Cadiz coastal buoy. The electric power expected in this location is *85.4* kW for AWS, *49* kW for Langlee, *60* kW for Oceantec, *57.02* kW for Oyster, *71.3* kW for OE Buoy, *52.7* kW for Wavebob, *676.4* kW for Wave Dragon and *1045.9* kW for SSG.

Table 4. Average electric power in kW for two onshore reference points in the bay of Cádiz, estimations corresponding to the characteristics of eight WEC devices.

Average Electric Power (in kW)		
POINTS		
WECs	**C. COASTAL B**	**SIMAR 6008050**
AWS	85.4	59.3
LANGLEE	49.0	41.4
OCEANTEC	60.0	52.0
OYSTER	57.02	45.2
OE BUOY	71.3	54.3
WAVEBOB	52.7	39.2
WAVE DRAGON	676.4	525.9
SSG	1045.9	820.7

In order to provide a more comprehensive picture of the geographical variations of the electric power estimated for each wave energy converter considered, the non-dimensional normalized wave power (P_{En}) was evaluated separately for each device in the reference points considered. Thus, the figure 7 illustrates the normalized electric energy provided by the offshore devices (Pelamis, Aqua Buoy and Langlee) in the reference points. Similar representations are illustrated in the figure 8 for Oceantec, Pontoon and OE Buoy. And the figure 9 for Wavebob and Wave Dragon. Figure10 shows the normalized electric energy provided by the onshore devices (AWS, Langlee, Oceantec, Oyster, OE Buoy, Wavebob, Wave Dragon and SSG).

The normalized wave power is expressed as:

$$P_{En} = \frac{P_E}{P_{ET\ max}}$$

(3)

in which P_E is the estimated electric power in the respective location for the device considered; and $P_{ET\ max}$ represents the maximum value from all the geographical locations estimated for total time for the same device.
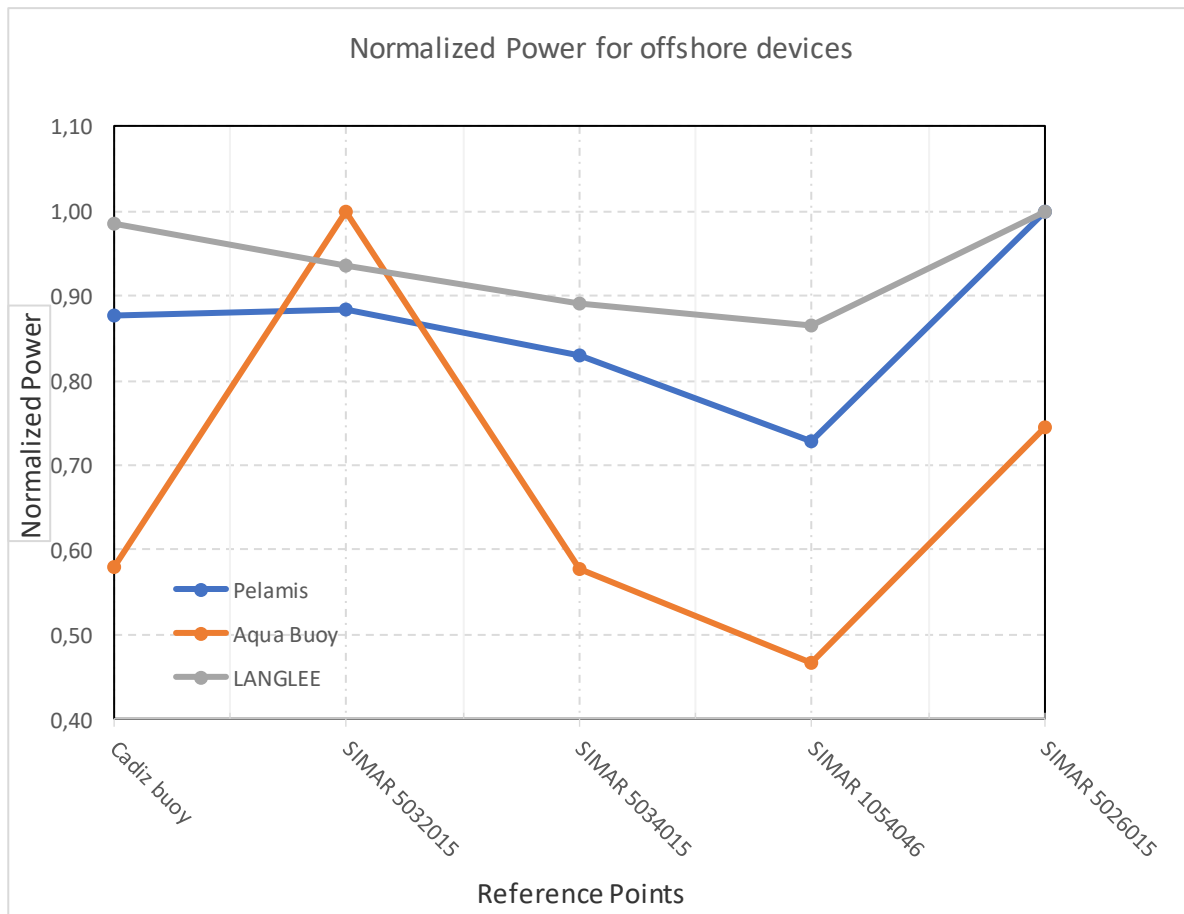
Fig. 7 Normalized electric power for the offshore devices, Pelamis, Aqua Buoy and Langlee in the reference points.

For Aqua Buoy the locations SIMAR 1054046 and SIMAR 5034015 appear to be the less energetic while the location SIMAR 5032015 is the most energetic. For Pelamis and Langlee the locations SIMAR 1054046 and SIMAR 5034015 appear to be also the less energetic while the location SIMAR 5026015 is the most energetic (figure 7).
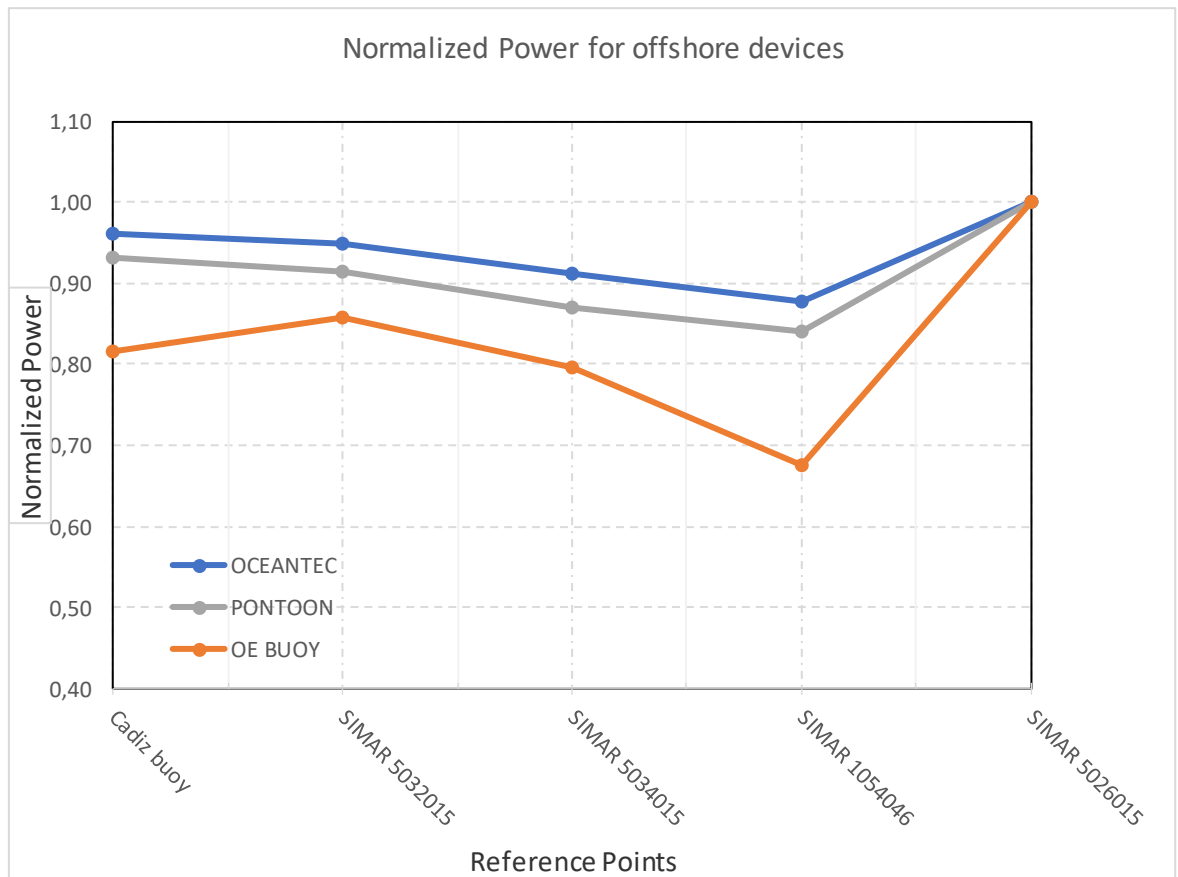
Fig. 8 Normalized electric power for the offshore devices, Oceantec, Pontoon and OE Buoy in the reference points.

For Oceantec, Pontoon and OE Buoy, the locations SIMAR 1054046 and SIMAR 5034015 appear to be the less energetic for the three ones, however OE Buoy shows a steeper low. The location SIMAR 5026015 is the most energetic (figure 8).
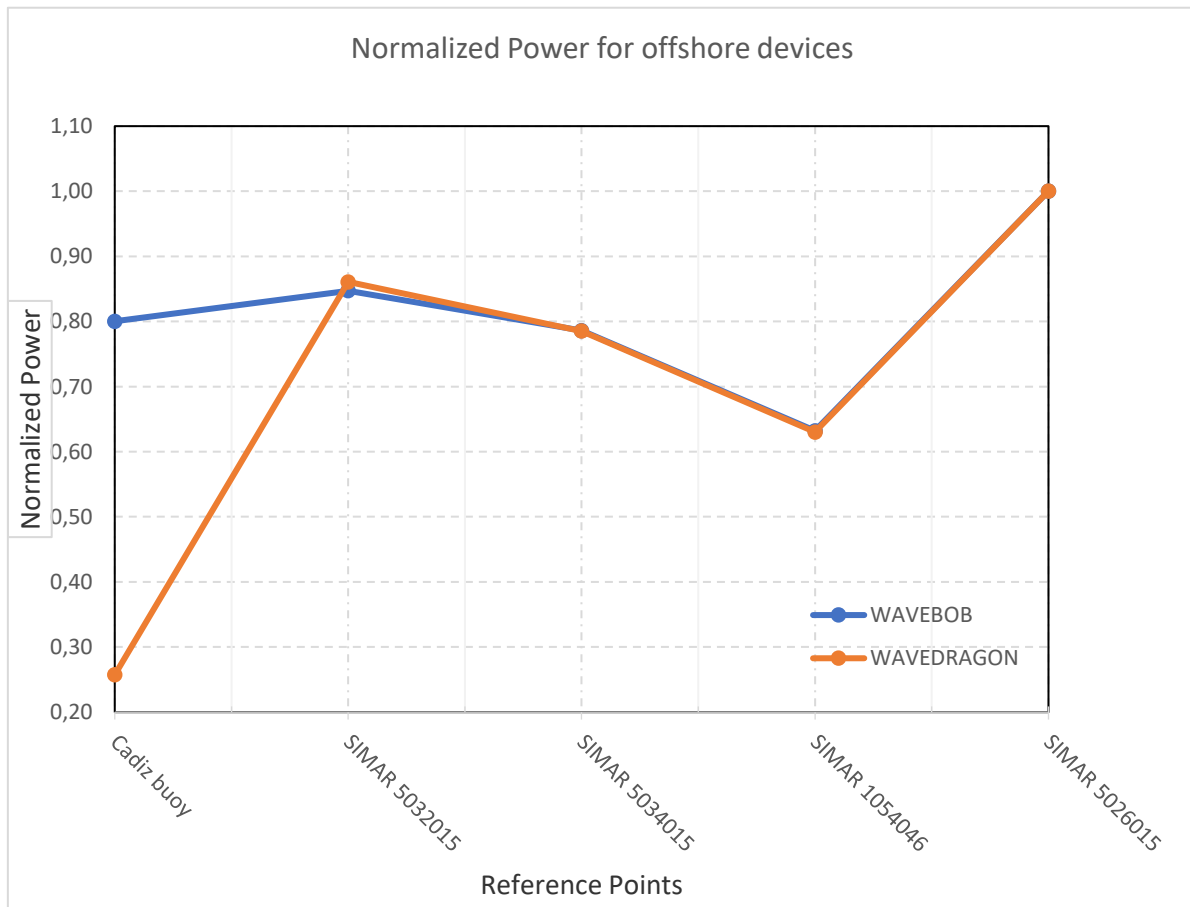
Fig. 9 Normalized electric power for the offshore devices, Wavebob and Wave Dragon in the reference points.

Wave Dragon presents a quite low energy value in the location Cádiz buoy, there is another low energy value in the location SIMAR 1054046. The most energetic location appears to be the location SIMAR 5026015. For Wavebob the less energetic location seems to be the location SIMAR 1054046 and the most energetic location, the SIMAR 5026015 (figure 9).
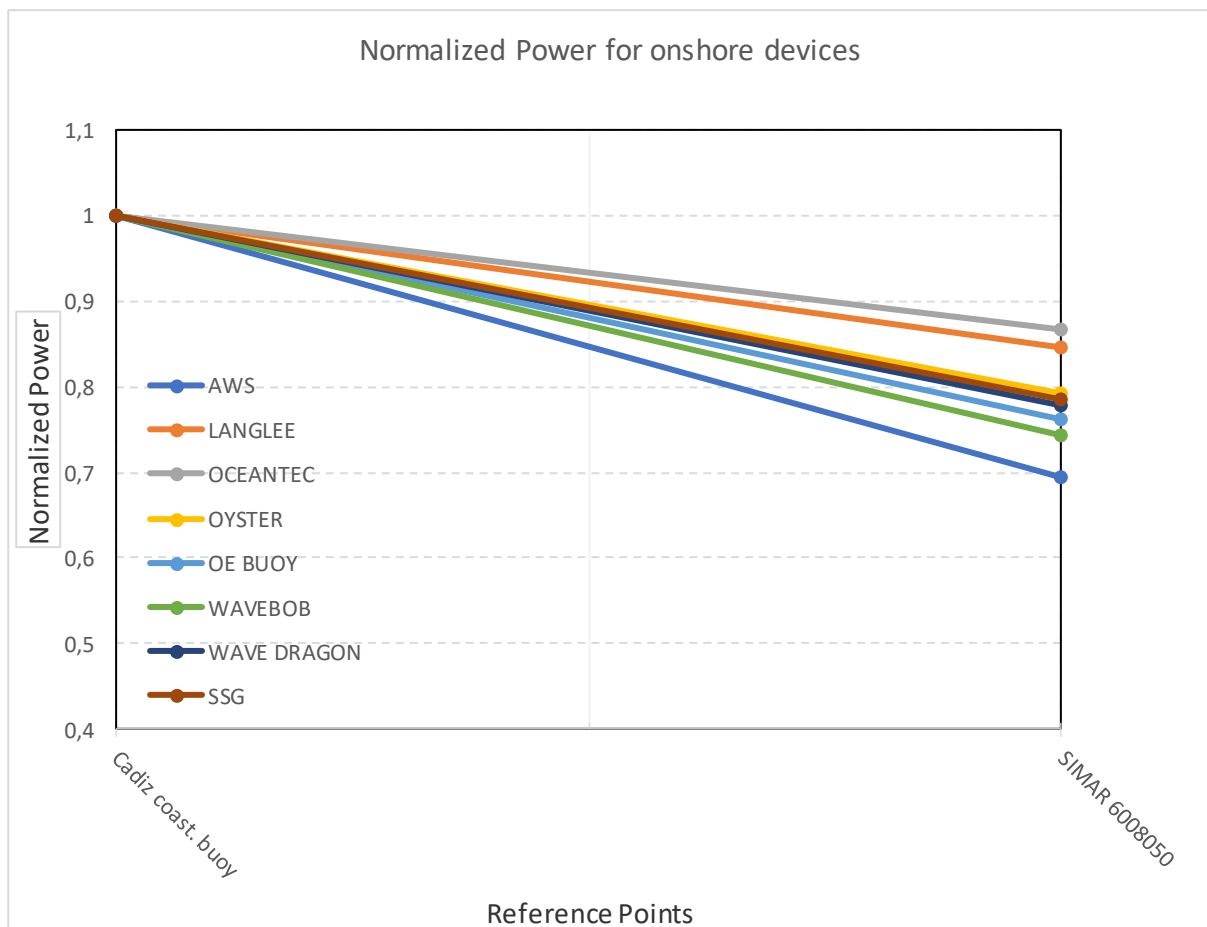
Fig. 10 Normalized electric power for the onhore devices, AWS, Langlee, Oceantec, Oyster, OE Buoy, Wavebob , Wave Dragon and SSG in the reference points.

For all the onshore devices studied, the location SIMAR 6008050 appear to be the less energetic while the location Cádiz coastal buoy is the most energetic (figure 10).

5. Discussion

Following the obtained in this work, in the offshore reference locations (table 3) at the Bay of Cádiz, the range of average electric power in kW for the different WECs is Pelamis [*61 84*] kW, Aqua Buoy [*18 38*] kW, AWS [*111 172*] kW, Oceantec [*101 115*] kW, Pontoon [*183 217*] kW, Wavebob [*62 98*] kW, Wave Dragon [*342 1329*] kW. In the onshore reference locations (table 4) at the Bay of Cádiz, the range of average electric power in kW for the different WECs is AWS [*59 85*] kW, Langlee [*41 49*] kW, Oyster [*45 57*] kW, OE Buoy [*54 71*] kW, Wavebob [*39 53*] kW, Wave Dragon [*526 676*] kW, SSG [*821 1046*] kW.

In the paper of Gonçalves et al. [8], the average electric power in different locations around the Canary Islands is obtained. The range of average electric power in kW for the different WECs is Aqua Buoy [*11 27*] kW, Wave Dragon [*365 479*] kW, Pelamis [*46 88*] kW. Comparing the maximum electric power of each offshore WECs at the bay of Cádiz and Canary Islands, it can be seen that Aqua Buoy's average electric power is *40.7*% higher in the bay of Cádiz than in the Canary Islands. Wave Dragon's average electric power is *177.45* % higher in the bay of Cádiz than in the Canary Islands. On the other hand, Pelamis average electric power is *4.76* % higher in the Canary Islands than in the bay of Cádiz.

In the work of Diaconu and Rusu [31], the performance provided by various technologies for wave energy conversion that would operate on the western side of the Black Sea is presented. The average electric power in kW for the WECs is Wave Dragon *392* kW, Pelamis *60* kW, Aqua Buoy *16* kW, AWS *60* kW, Oceantec *96* kW, Pontoon *164* kW, Wavebob *55* kW. Making a comparison of the maximum electric power of each offshore WECs at the bay of Cádiz and the western side of Black Sea, for all the WECs considered, the bay of Cádiz obtained higher values of electric power than the Black Sea. Being the average electric power of Wave Dragon is *239%* higher in the bay of Cádiz, Pelamis *40%*, Aqua Buoy *137.5%*, AWS *186.67%*, Oceantec *19.79%*, Pontoon *32.31%* and Wavebob *78.18%*.

In the paper of Silva et al. [17], the output of five different technologies for the conversion of wave energy is assessed in some relevant locations from the Portuguese nearshore. The range of average electric power in kW for the different offshore WECs, in those locations, is Aqua Buoy [*30 36*] kW and Pelamis [*86 102*] kW. The range of average electric power in kW for the different onshore WECs, in those locations, is Oyster [*71 107*] kW, Wave Dragon [*599 905*] kW, and SSG [*2040 3025*] kW. Comparing the maximum electric power of each offshore WECs at the bay of Cádiz and the Portuguese continental coast, for Aqua Buoy is *5.5%* higher at the bay of Cádiz than at the Portuguese coast, for Pelamis is *21.43%* higher in the Portuguese coast than at the bay of Cádiz. Making a comparison of the maximum electric power of each onshore WECs at the bay of Cádiz and Portuguese continental coast, the Portuguese continental coast presents higher values of electric power than the bay of Cádiz. Being the average electric power of Wave Dragon is 33.88 % higher on the Portuguese coast, of Oyster *87.72%*, and of SSG *189.2%*.

In the work of Rusu [39], the performances of three WEC types in three different groups of coastal environments: the western Iberian nearshore, islands, and an enclosed environment is studied. Regarding northwestern Spain, the range of average electric power in kW for the different offshore WECs is Oceantec [*94 107*] kW, Pelamis [*114 127*] kW, Pontoon [*220 239*] kW, Wave Dragon [*2037 2198*] kW. Comparing the maximum electric power of each offshore WECs at the bay of Cádiz and in the northwestern of Spain, for Oceantec is *7.48%* higher at the bay of Cádiz than in the northwestern of Spain, for Pelamis, Pontoon and Wave Dragon is higher in the northwestern of Spain than at the bay of Cádiz, being *51.2%*, *10.14%*, and *65.39%* respectively. With regard to the Portuguese coast, the range of average electric power in kW for the different offshore WECs is Pelamis [*79 102*] kW, AWS [*247 296*] kW, Aqua Buoy [*29 36*] kW, Wave Dragon [*1153 1475*] kW. Making a comparison of the maximum electric power of each offshore WECs at the bay of Cádiz and in the Portuguese coast, for Aqua Buoy is *5.55%* higher at the bay of Cádiz than in the Portuguese coast, for Pelamis, AWS and Wave Dragon is higher in the Portuguese coast than at the bay of Cádiz, being *21.43%*, *72.09%*, and *10.98%* respectively. With respect to the Canary Islands, the range of average electric power in kW for the different offshore WECs is Pelamis [*65 90*] kW, AWS [*255 277*] kW, Aqua Buoy [*24 32*] kW, Wavebob [*87 106*] kW. Comparing the maximum electric power of each offshore WECs at the bay of Cádiz and in the Canary Islands, for Aqua Buoy is *18.75%* higher at the bay of Cádiz than in the Canary Islands, for Pelamis, AWS, and Wavebob is higher in the Canary Islands than at the bay of Cádiz, being *7.14%*, *61.04%*, and *8.16%* respectively. Regarding the Black Sea, the range of average electric power in kW for the different offshore WECs is Pelamis *60* kW, Aqua Buoy *16* kW, and Wave Dragon *391* kW. Making a comparison of the maximum electric power of each offshore WECs at the bay of Cádiz and the western side of Black Sea, for all the WECs considered, the bay of Cádiz obtained higher values of electric power than the Black Sea. Being the average electric power of Pelamis is *40%* higher in the bay of Cádiz, Aqua Buoy is *137.5%*, Wave Dragon *239.90%*. With regards to the North Sea at Fino station, the range of

average electric power in kW for the different offshore WECs is Pelamis *70* kW, Aqua Buoy *12* kW, and Wave Dragon *735* kW. Comparing the maximum electric power of each offshore WECs at the bay of Cádiz and the North Sea at Fino station, for all the WECs considered, the bay of Cádiz obtained higher values of electric power than the North Sea at Fino station. Being the average electric power of Pelamis is *20*% higher in the bay of Cádiz, Aqua Buoy *216.67*% and Wave Dragon *80.82*%.

In the paper of Vannucchi and Cappietti [40], the performances of different WECs have been evaluated in the Italian coastal areas, the coast of Tuscany, Liguria, Sardinia, and Sicily. Regarding Italian coastal areas, the range of average electric power in kW for the different offshore WECs is Aqua Buoy [*3 21*] kW, Pelamis [*7 49*] kW, AWS [*7 99*] kW, and Wave Dragon [*227 540.4*] kW and for the onshore WEC Oyster [*8 48*] kW. Making a comparison of the maximum electric power of each offshore WECs at the bay of Cádiz and in the Italian coastal areas, for all the WECs considered, the bay of Cádiz obtained higher values of electric power than Italian coastal areas. Being the average electric power of Aqua Buoy is *80.95*% higher in the bay of Cádiz, Pelamis *71.43*%, AWS *73.73*%, Wave Dragon *145.93*%, and Oyster *18.75*%.

In the work of Rusu and Guedes [41], three WECs performance around Madeira Islands is presented. With regard to Madeira Islands, the range of average electric power in kW for the different offshore WECs is Pelamis [*105 135*] kW, Wave Dragon [*1147 1644*] kW, and Aqua Buoy [*40 50*] kW. Comparing the maximum electric power of each offshore WECs at the bay of Cádiz and Madeira Islands, for all the WECs considered, Madeira Islands obtained higher values of electric power. Being the average electric power of Pelamis is *60.71*% higher in the Madeira Islands, Aqua Buoy is *31.58*%, and Wave Dragon is *23.70*%.

In the paper of Bozzi and at al. [42], the performance of three waves energy converters is estimated for two of the most energetic Italian locations. The sites are Alghero, on the western coast of Sardinia, and Mazara del Vallo, on the Sicily Strait. The average electric power in kW for the WECs is Aqua Buoy [*9 22*] kW, Pelamis [*32 71*] kW, and Wave Dragon [*270 616*] kW. Making a comparison of the maximum electric power of each offshore WECs at the bay of Cádiz and in the Italian locations, for all the WECs considered, the bay of Cádiz obtained higher values of electric power than Italian locations. Being the average electric power of Aqua Buoy is *72.73*% higher in the bay of Cádiz, Pelamis *18.31*% and Wave Dragon *115.75*%.

In order to analyze the variability of the energy capture in the studied area of the bay of Cádiz, a comparison of the power obtained by each WECs in the different points of reference is carried out.

Focusing on offshore devices, table 3, for Pelamis, the maximum difference in power is obtained between SIMAR 5026015 and SIMAR 105406 points, being *37.35*%. And the minimum difference is obtained between SIMAR 5032015 and Cádiz buoy points, being of *0.8*%. The difference between the other reference points is among these quantities. For Aqua Buoy, the maximum power difference is given between SIMAR 5032015 and SIMAR 1054046 points, being *114.124*%. And the minimum difference is obtained between Cádiz buoy and SIMAR 5032015 points, being of *0.45*%. The difference between the other reference points is among these quantities. For AWS, the maximum power difference is given between SIMAR 5026015 and SIMAR 1054046 points, being *55.38*%. And the minimum difference is obtained between Cádiz buoy and SIMAR 5032015 points, being of *3.36*%. The difference between the other reference points is among these quantities. For Langlee, the maximum power difference is given between SIMAR 5026015 and SIMAR 1054046 points, being *15.69*%. And the minimum difference is obtained between the Cádiz buoy and SIMAR 5032015 points, being *1.38*%. The difference between the other reference points is among

these quantities. For Oceantec, the maximum power difference is given between SIMAR 5026015 and SIMAR 1054046 points, being *13.95%*. And the minimum difference is obtained between Cádiz buoy and SIMAR 5032015 points, being *1.37%*. The difference between the other reference points is among these quantities. For Pontoon, the maximum power difference is given between SIMAR 5026015 and SIMAR 1054046 points, being *18.78%*. And the minimum difference is obtained between Cádiz buoy and SIMAR 5032015 points, being *1.91%*. The difference between the other reference points is among these quantities. For OE Buoy, the maximum power difference is given between SIMAR 5026015 and SIMAR 1054046 points, being *48.31%*. And the minimum difference is obtained between Cádiz buoy and SIMAR 5032015 points, being *5.02%*. The difference between the other reference points is among these quantities. For Wavebob, the maximum power difference is given between SIMAR 5026015 and SIMAR 1054046 points, being *58.23%*. And the minimum difference is obtained between Cádiz buoy and SIMAR 5032015 points, being *1.82%*. The difference between the other reference points is among these quantities. For Wave Dragon, the maximum power difference is given between SIMAR 5026015 and Cádiz buoy points, being *288.40%*. And the minimum difference is obtained between SIMAR 5034015 and SIMAR 5032015 points, being *9.58%*. The difference between the other reference points is among these quantities.

Regarding onshore devices, the power difference between the two studied points, Cádiz coastal buoy and SIMAR 6008050 points is: for AWS of *44.01%*, for Langlee of *18.35%*, for Oceantec of *15.38%*, for Oyster of *26.15%*, for OE Buoy of *31.31%*, for Wavebob of *34.44%*, for Wave Dragon of *28.62%* and for SSG of *27.44%*.

With regard to the paper of Gonçalves et al. [8], the maximum power difference at the different locations studied around Canary Island is: for Aqua Buoy of *145.45%*, for Wave Dragon of *31.23%* and for Pelamis of *91.30%*. With respect to the paper of Silva et alt. (Dina), the maximum power difference at the different locations studied in the Portuguese nearshore is: for Aqua Buoy of *20%*, for Pelamis of *18.60%*, for Oyster of *50.70%*, for Wave Dragon of *51.09%* and for SSG of *48.28%*. Regarding the work of Rusu [39], the maximum power difference at the different locations studied in the northwestern of Spain is: for Oceantec *13.83%*, for Pelamis *11,40%*, for Potoon *8.64%*, and for Wave Dragon *7.90%*. The maximum power difference at the different locations studied on the Portuguese coast is: for Pelamis *29.11%*, for AWS *19.84%*, for Aqua Buoy *24.14%*, for Wave Dragon *27.93%*. The maximum power difference at the different locations studied in the Canary Islands is: for Pelamis *38.46%*, for AWS *8.63%*, for Aqua Buoy *33.33%*, for Wavebob *21.84%*. With regard to the paper of Vannucchi and Cappietti [40], the maximum power difference at the different locations studied in Italian coastal areas is: for Aqua Buoy *600%*, for Pelamis *600%*, for AWS *1314.29%*, for Wave Dragon *138.06%*, and for Oyster *500%*. With respect to the work of Rusu and Guedes [41], the maximum power difference at the different locations studied around Madeira Islands is: for Aqua Buoy *25%*, for Pelamis *28.57%*, and for Wave Dragon *43.33%*. Regarding the paper of Bozzi and at al. [42], the maximum power difference at the different locations studied in Italy: for Aqua Buoy *144.44%*, for Pelamis *121.88%*, and for Wave Dragon *128.15%*.

Making a comparison between the bay of Cádiz and the different locations studied in the before cited papers, it can be observed that the variability of power obtained in the bay of Cádiz is similar to the variation obtained by them. Moreover, it is much less than in the coastal Italian locations studied in the work of Vannucchi and Cappietti [40].

6.   Conclusions

A medium-term evaluation of the wave conditions (corresponding to the time interval 2010-2014) was presented in the present work considering several reference locations in the bay of Cádiz. This was made using the data available from the Spanish Agency Puertos del Estado.

On this basis, the efficiency of nine energy converters, covering the full scale from the point of view of their location (offshore and onshore), was evaluated in the bay of Cádiz. The estimations were made by diagrams for the bivariate distributions of the occurrences corresponding to the sea states defined by significant wave height and energy period.

A good agreement between the characteristics of the power matrices of the wave energy converters operating in a certain place and the diagrams for the bivariate distributions of the sea states occurrences corresponding to the considered location represent a key issue in selecting the most appropriate location for a WEC. An example is given by the reference location Cádiz coastal buoy, onshore point, in which Wave Dragon would produce more energy (*676.4* kW) than in the offshore location Cádiz buoy (*342.1* kW).

Following the results presents in this work, the bay of Cádiz has obtained higher electric power than the Canary Islands for Aqua Buoy and Wave Dragon, and higher than the northwester of Spain for Oceantec. Moreover, the bay of Cádiz has presented higher values of electric power than the western side of the Black Sea and the North Sea at Fino station for all the WECs studied. What is more, the bay of Cádiz has reached higher values of electric power than the locations studied around Italy for all WECs studied. The variability of power obtained in the bay of Cádiz is similar to the variation obtained in other locations studied (the Canary Islands, Portuguese nearshore, Madeira Islands, northwestern of Spain). Moreover, it is much less than in the areas of Italy. Taking into consideration this study, it can be said that the bay of Cádiz is a suitable place for wave energy extraction.

It is necessary to consider that the non-technical factors should also be considered to reach the final decisions about the proper location and type of WECs to install. Furthermore, the concepts used are ones that have information available in the literature, which is useful to provide a general order of magnitude of the expected contribution. However, some of them are not commercially available for deployment, so a more detailed study will be required after the first level of decisions are made.

Thinking in future studies, the first thing to do would be to consult the commercial availability of the WECs. In the second place, studying the possibility of establishing a WEC farm in the bay of Cádiz, taking into account the use of maritime space by other activities and the design of the possible WECs farm. Next studies would be some techno-economic analysis to cost the WEC energy converted, some analysis of the correlation between converted wave power and electricity demand, the possibility of optimization of the WEC for the chosen locations, and so on.

Appendix A

In this appendix, the power matrix of the different WECs system used in this research is shown.

Table A1. Power matrix (in kW) for the wave energy converter Wave Dragon [31]

Power matrix (in kW)													
Hs (m)	$T_e(s)$												
	5	**6**	**7**	**8**	**9**	**10**	**11**	**12**	**13**	**14**	**15**	**16**	**18**
1	160	250	360	360	360	360	360	360	320	280	250	220	180
2	640	700	840	900	1190	1190	1190	1190	1070	950	830	710	590
3	0	1450	1610	1750	2000	2620	2620	2620	2360	2100	1840	1570	1310
4	0	0	2840	3220	3710	4200	5320	5320	4430	3930	3440	2950	2460
5	0	0	0	4610	5320	6020	7000	7000	6790	6090	5250	3950	3300
6	0	0	0	0	6720	7000	7000	7000	7000	7000	6860	5110	4200
7	0	0	0	0	0	7000	7000	7000	7000	7000	7000	6650	5740

Table A2. Power matrix (in kW) for the wave energy converter Archimedes Wave Swing [31]

Power matrix (in kW)																			
Hs (m)	$Tp(s)$																		
	5	**5.5**	**6**	**6.5**	**7**	**7.5**	**8**	**8.5**	**9**	**9.5**	**10**	**10.5**	**11**	**11.5**	**12**	**12.5**	**13**	**13.5**	**14**	**14.5**
1	2	7	13	19	26	34	41	48	58	68	81	93	105	118	131	144	153	163	183	203
1.5	4	15	28	41	56	72	85	99	121	143	173	203	226	248	266	285	309	334	357	380
2	8	26	49	73	100	127	150	172	210	247	292	337	366	395	418	442	482	523	543	563
2.5	15	43	78	113	159	205	234	263	320	376	438	499	531	563	603	643	675	708	741	774
3	25	61	111	161	227	293	339	386	453	521	600	680	722	765	827	888	897	906	945	984
3.5	35	92	155	218	305	391	454	517	605	694	772	851	913	975	1036	1096	1119	1141	1163	1185
4	35	114	194	273	380	486	572	659	776	894	961	1027	1103	1179	1227	1275	1316	1357	1365	1374
4.5	0	0	235	332	479	626	722	819	957	1096	1168	1240	1320	1401	1449	1497	1547	1598	1590	1583
5	0	0	280	400	592	784	899	1014	1144	1274	1380	1487	1569	1651	1691	1731	1785	1838	1807	1777
5.5	0	0	320	432	641	849	1033	1216	1331	1446	1568	1690	1778	1867	1919	1970	1977	1984	1994	2005
6	0	0	0	0	680	944	1155	1367	1495	1623	1759	1895	1963	2072	2137	2202	2205	2207	2226	2246
6.5	0	0	0	0	720	1123	1335	1547	1678	1809	1963	2116	2200	2284	2332	2380	2425	2470	2452	2434

Table A3. Power matrix (in kW) for the wave energy converter Langlee [31]

Power matrix (in kW)													
Hs(m)	$Tp(s)$												
	4	**5**	**6**	**7**	**8**	**9**	**10**	**11**	**12**	**13**	**14**	**15**	**16**
1	19	29	47	57	52	37	29	20	17	13	9	7	7
1.5	42	63	92	111	109	65	56	38	29	22	19	13	11
2	66	99	151	201	165	105	85	59	52	41	23	24	19
2.5	0	160	242	262	226	166	118	83	70	57	39	29	26
3	0	213	319	372	327	211	152	116	94	75	66	45	42
3.5	0	0	436	503	408	293	203	148	115	93	75	58	44
4	0	0	554	540	521	355	261	192	144	123	84	81	56
4.5	0	0	645	746	587	379	302	236	190	154	106	90	74
5	0	0	796	926	695	486	341	287	211	168	136	111	94
5.5	0	0	0	955	808	603	430	343	231	201	150	120	97
6	0	0	0	1161	957	642	481	329	289	212	172	145	111
6.5	0	0	0	1476	1039	702	488	397	312	237	204	153	120
7	0	0	0	1665	1197	879	612	466	385	252	223	181	146

Table A4. Power matrix (in kW) for the wave energy converter Oceantec [31]

	Power matrix (in kW)												
	Tp(s)												
Hs(m)	6	7	8	9	10	11	12	13	14	15	16	17	18
1	85	87	59	39	25	16	10	7	5	3	2	2	1
1.5	191	196	133	89	57	36	23	15	10	7	5	3	3
2	339	348	234	158	101	64	41	27	18	12	9	6	4
2.5	500	500	364	245	158	101	65	42	28	19	13	10	7
3	500	500	500	337	228	145	93	61	41	28	19	14	10
3.5	500	500	500	420	309	196	127	83	55	38	26	19	13
4	500	500	500	500	401	258	166	109	72	49	34	24	18
4.5	500	500	500	500	500	326	210	138	92	62	43	31	22
5	500	500	500	500	500	383	259	170	113	77	54	38	27
5.5	500	500	500	500	500	389	308	205	137	93	65	46	33

Table A5. Power matrix (in kW) for the wave energy converter Pelamis [31]

	Power matrix (in kW)												
Hs(m)	Te(s)												
	5	5.5	6	6.5	7	7.5	8	9	10	11	12	13
0.5	0	0	0	0	0	0	0	0	0	0	0	0
1	0	22	29	34	37	38	38	35	29	23	0	0
1.5	32	50	65	76	83	86	86	78	65	53	42	33
2	57	88	115	136	148	153	152	138	116	93	74	59
2.5	89	138	180	212	231	238	238	216	181	146	116	92
3	129	198	260	305	332	340	332	292	240	210	167	132
3.5	0	270	354	415	438	440	424	377	326	260	215	180
4	0	0	462	502	540	546	530	475	384	339	267	213
4.5	0	0	544	635	642	648	628	562	473	382	338	266
5	0	0	0	739	726	731	707	670	557	472	369	328
5.5	0	0	0	750	750	750	750	737	658	530	446	355
6	0	0	0	0	750	750	750	750	711	619	512	415
6.5	0	0	0	0	750	750	750	750	750	658	579	481
7	0	0	0	0	0	750	750	750	750	750	613	525
7.5	0	0	0	0	0	0	750	750	750	750	686	593
8	0	0	0	0	0	0	0	750	750	750	750	625

Table A6. Power matrix (in kW) for the wave energy converter Pontoon [31]

Power matrix (in kW)													
Hs(m)	Tp(s)												
	4	5	6	7	8	9	10	11	12	13	14	15	16
1	180	166	153	171	125	87	72	65	85	85	37	29	16
1.5	223	195	157	148	261	192	223	139	155	155	74	67	46
2	0	0	214	227	396	335	237	235	172	138	115	104	70
2.5	0	0	0	440	598	514	379	342	204	169	142	128	95
3	0	0	0	681	801	735	594	486	199	174	151	134	121
3.5	0	0	0	904	1035	949	788	617	239	209	183	164	146
4	0	0	0	1131	1269	1163	982	743	285	248	216	195	175
4.5	0	0	0	1358	1488	1374	1187	869	330	287	250	225	201
5	0	0	0	1585	1712	1585	1392	988	380	334	285	263	226
5.5	0	0	0	1812	1937	1798	2138	1107	429	381	323	301	261
6	0	0	0	2040	2162	2010	2884	1234	439	416	361	336	295
6.5	0	0	0	2267	2386	2221	3143	1360	449	450	406	372	329
7	0	0	0	2494	2611	2433	3619	1483	506	464	451	408	363

Table A7. Power matrix (in kW) for the wave energy converter OE buoy [31]

Power matrix (in kW)													
Hs (m)	Tp(s)												
	4	5	6	7	8	9	10	11	12	13	14	15	16
1	8	17	27	42	56	59	52	44	40	38	40	38	30
1.5	17	39	61	96	126	132	117	99	89	87	89	85	66
2	30	69	108	170	224	235	208	177	159	154	159	151	118
2.5	47	108	169	266	350	368	324	276	249	241	248	236	185
3	68	155	244	383	504	530	467	398	358	347	357	340	266
3.5	93	212	332	521	686	721	636	542	487	472	486	463	362
4	121	276	433	680	896	942	831	708	636	616	634	605	473
4.5	154	350	548	861	1130	1190	1050	896	805	780	803	765	599
5	190	432	677	1060	1400	1470	1300	1110	994	963	991	945	739
5.5	0	523	819	1290	1690	1780	1570	1340	1200	1170	1200	1140	894
6	0	622	975	1530	2020	2120	1870	1590	1430	1390	1430	1360	1060
6.5	0	730	1140	1800	2370	2490	2190	1870	1680	1630	1670	1600	1250
7	0	847	1330	2080	2750	2880	2540	2170	1950	1890	1940	1850	1450

Table A8. Power matrix (in kw) for the wave energy converter Wavebob [31

							Power matrix (in kW)						
	Tp(s)												
Hs(m)	**4**	**5**	**6**	**7**	**8**	**9**	**10**	**11**	**12**	**13**	**14**	**15**	**16**
1	6	11	19	25	30	44	50	53	44	34	22	20	17
1.5	13	25	43	55	68	90	102	92	91	66	65	45	37
2	24	45	65	100	121	153	175	151	122	126	87	61	58
2.5	0	65	104	141	191	179	243	255	190	181	135	99	83
3	0	96	137	205	244	357	293	353	260	248	184	137	120
3.5	0	0	192	254	291	431	385	424	314	285	239	222	172
4	0	0	256	366	403	551	536	531	473	420	289	268	179
4.5	0	0	327	418	574	678	708	665	509	415	386	244	249
5	0	0	358	514	658	824	828	618	638	512	452	384	333
5.5	0	0	0	610	774	880	936	905	805	603	456	397	311
6	0	0	0	711	952	974	1000	838	886	648	501	503	396
6.5	0	0	0	788	1000	1000	1000	979	1000	727	577	435	424
7	0	0	0	871	1000	1000	1000	1000	1000	959	748	574	472

Table A9. Power matrix (in kW) for the wave energy converter Oyster [3]

				Power matrix (in kW)					
Hs(m)	Te(s)								
	5	**6**	**7**	**8**	**9**	**10**	**11**	**12**	**13**
0.5	0	0	0	0	0	0	1	3	3
1	20	30	38	42	44	44	45	47	45
1.5	80	85	92	97	102	103	104	100	104
2	140	147	152	158	155	155	160	161	156
2.5	192	197	208	202	203	209	211	201	204
3	241	237	237	241	243	230	236	231	235
3.5	0	271	272	269	268	267	270	260	260
4	0	291	290	290	280	287	276	278	277
4.5	0	291	290	290	280	287	276	278	277
5	0	0	290	290	280	287	276	278	277
5.5	0	0	290	290	280	287	276	278	277
6	0	0	290	290	280	287	276	278	277

Table A10. Power matrix (in kW) for the wave energy converter Aqua Buoy [31]

Power matrix (in kW)													
Hs(m)	Tp(s)												
	5	6	7	8	9	10	11	12	13	14	15	16	17
1	0	0	8	11	12	11	10	8	7	0	0	0	0
1.5	0	13	17	25	27	26	23	19	15	12	12	12	7
2	0	24	30	44	49	47	41	34	28	23	23	23	12
2.5	0	37	47	69	77	73	64	54	43	36	36	36	19
3	0	54	68	99	111	106	92	77	63	51	51	51	27
3.5	0	0	93	135	152	144	126	105	86	70	70	70	38
4	0	0	0	122	176	198	173	164	137	112	91	91	49
4.5	0	0	0	223	250	239	208	173	142	115	115	115	62
5	0	0	0	250	250	250	250	214	175	142	142	142	77
5.5	0	0	0	250	250	250	250	250	211	172	172	172	92

Table A11. Power matrix (in kW) for the wave energy converter SSG [3]

Power matrix (in kW)														
Hs(m)	Te(s)													
	5	5.5	6	6.5	7	7.5	8	8.5	9	9.5	10	10.5	11	11.5
0.5	99.00	109.000	119.000	129.000	139.000	149.000	159.000	169.000	179.000	189.000	198.000	208.000	218.000	228.000
1	397.00	437.000	476.000	516.000	556.000	595.000	635.000	675.000	715.000	754.000	794.000	833.000	873.000	913.000
1.5	893.00	982.000	1072.000	1161.000	1250.000	1340.000	1429.000	1518.000	1608.000	1697.000	1786.000	1875.000	1965.000	2054.000
2	1588.00	1746.000	1905.000	2064.000	2223.000	2381.000	2540.000	2699.000	2858.000	3016.000	3175.000	3334.000	3493.000	3651.000
2.5	2481.00	2729.000	2977.000	3225.000	3473.000	3721.000	3969.000	4217.000	4465.000	4713.000	4961.000	5209.000	5457.000	5705.000
3	3572.000	3929.000	4287.000	4644.000	5001.000	5358.000	5715.000	6073.000	6430.000	6787.000	7144.000	7501.000	7859.000	8216.000
3.5	4862.00	5348.000	5834.000	6.321	6807.000	7203.000	7779.000	8265.000	8751.000	9238.000	9724.000	10.210	10.695	11.183
4	6350.00	6985.000	7620.000	8.256	8891.000	9526.000	10.161	10.796	11.431	12.066	12.701	13.336	13.971	14.606
4.5	8037.00	8841.000	9645.000	10.448	11.252	12.056	12.860	13.663	14.467	15.271	16.074	16.878	17.682	18.486
5	9923.00	10.915	11.907	12.899	13.892	14.884	15.876	16.868	17.860	18.853	19.845	20.000	20.000	20.000
5.5	12.006	13.207	14.407	15.608	16.809	18.009	19.210	20.000	20.000	20.000	20.000	20.000	20.000	20.000
6	14.288	15.717	17.146	18.575	20.000	20.000	20.000	20.000	20.000	20.000	20.000	20.000	20.000	20.000
6.5	16.769	18.446	20.000	20.000	20.000	20.000	20.000	20.000	20.000	20.000	20.000	20.000	20.000	20.000
7	19.448	20.000	20.000	20.000	20.000	20.000	20.000	20.000	20.000	20.000	20.000	20.000	20.000	20.000
7.5	20.000	20.000	20.000	20.000	20.000	20.000	20.000	20.000	20.000	20.000	20.000	20.000	20.000	20.000
8	20.000	20.000	20.000	20.000	20.000	20.000	20.000	20.000	20.000	20.000	20.000	20.000	20.000	20.000

APPENDIX B

In this appendix, figures of the different WECs system used in this research are shown.

Fig. 7 Wave dragon [33]

Fig. 8 Pelamis [34]

Fig. 9 AquaBuoy [35]

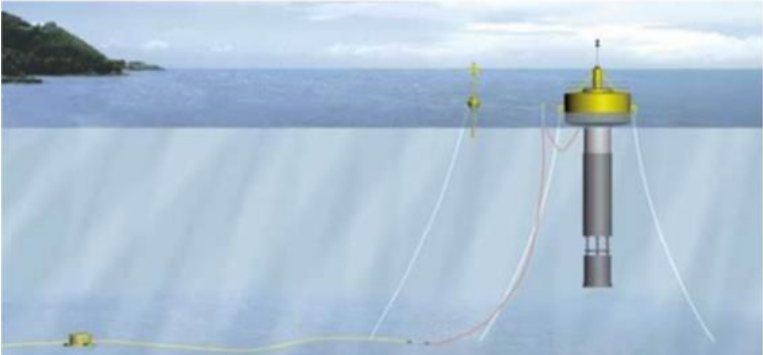**Fig. 10** Archimedes Wave Swing [36]

Fig. 11 Langlee [32]
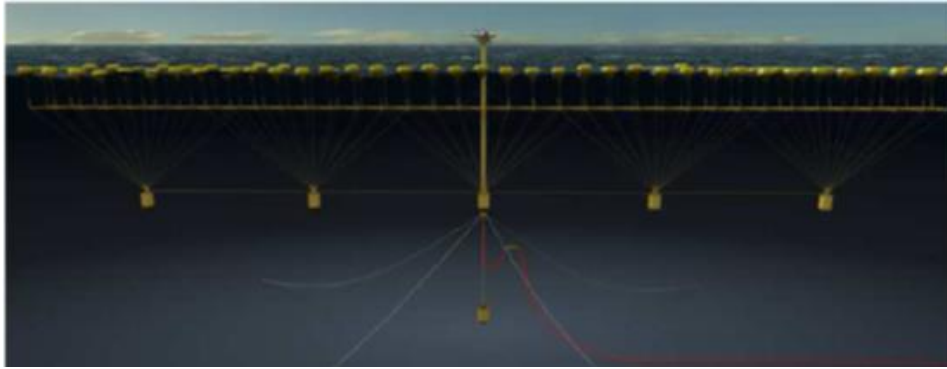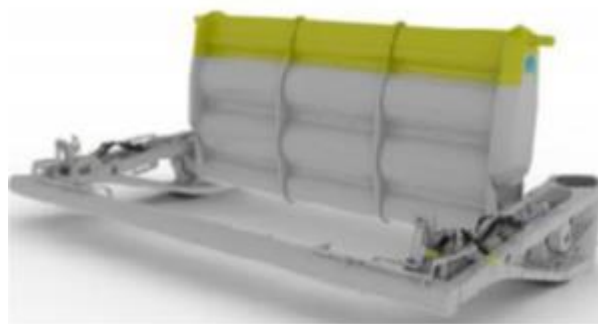

Fig. 12 Oceantec [37]

Fig. 13 OE buoy [32]

Fig. 14 Pontoon [32]

Fig. 15 Oyster [32]

Fig. 16 Wavebob [32]

Fig. 17 SSG [38]

REFERENCES

[1]   Soares C. G., Bento, A. R., Gonçalves, M., Silva, D., Martinho, P., 2014. Numerical evaluation of the wave energy resource along the Atlantic European coast. *Computers & Geosciences*, 71, 37-49. https://doi.org/10.1016/j.cageo.2014.03.008

[2]   Silva, D., Bento, A. R., Martinho, P., Soares, C. G., 2015. High resolution local wave energy modelling for the Iberian Peninsula. *Energy*, 91,1099-1112; 94, 857-858. https://doi.org/10.1016/j.energy.2015.11.033

[3]   Silva, D., Martinho, P., Soares, C. G., 2018. Wave energy distribution along the Portuguese continental coast based on a thirty three years hindcast. *Renewable Energy*, 127(4), 1067-1075. https://doi.org/10.1016/j.renene.2018.05.037

[4]   Rusu, E., Pilar, P., Soares, C. G., 2008. Evaluation of the Wave Conditions in Madeira Archipelago with Spectral Models. *Ocean Engineering*, 35(13), 1357-1371. https://doi.org/10.1016/j.oceaneng.2008.05.007

[5]   Iglesias, G., Carballo, R., 2011. Wave resource in El Hierro—an island towards energy self-sufficiency. *Renewable Energy*, 36, 689-698. https://doi.org/10.1016/j.renene.2010.08.021

[6]   Rusu, L., Soares, C. G., 2012. Wave energy assessments in the Azores islands. *Renewable Energy*, 45, 183–196. https://doi.org/10.1016/j.renene.2012.02.027

[7]   Sierra, J.P., González-Marco, D., Sospedra, J., Gironella, X., Mösso, C., Sánchez-Arcilla, A., 2013. Wave energy resource assessment in Lanzarote (Spain). *Renewable Energy*, 55, 480-489. https://doi.org/10.1016/j.renene.2013.01.004

[8]   Gonçalves, M., Martinho, P., Soares, C. G., 2014. Assessment of wave energy in the Canary Islands. *Renewable Energy*, 68,774-784. https://doi.org/10.1016/j.renene.2014.03.017

[9]   Ponce de León S., Orfila A., Simarro G., 2015. Wave energy in the Balearic Sea. Evolution from a 29 years spectral wave hindcast. *Renewable Energy*, 82, 1192-1200. https://doi.org/10.1016/j.renene.2015.07.076

[10]   Bernardino, M., Rusu, L., Soares, C. G., 2017. Evaluation of the wave energy resources in the Cape Verde Islands. *Renewable Energy*, 101, 316-326. https://doi.org/10.1016/j.renene.2016.08.040

[11]   Silva, D., Rusu, E., Soares, C. G., 2016. High-resolution wave energy assessment in shallow water accounting for tides. *Energies*, 9(9), 761-779. https://doi.org/10.3390/en9090761

[12]   Rusu, E., Soares, C. G., 2013. Coastal Impact Induced by a Pelamis Wave Farm Operating in the Portuguese Nearshore. *Renewable Energy*, 58, 34-49. https://doi.org/10.1016/j.renene.2013.03.001

[13]   Silva, D., Rusu, E., Soares, C. G., 2018. The effect of a wave energy farm protecting an aquaculture installation. *Energies*, 11(8), 2109. https://doi.org/10.3390/en11082109

[14]   Monteforte, M., Re, C. L., Ferreri, G. B., 2015. Wave energy assessment in Sicily (Italy). *Renewable Energy*, 78, 276-287. https://doi.org/10.1016/j.renene.2015.01.006

[15]   Farkas, A., Degiuli, N., Martić, I., 2019. Assessment of offshore wave energy potential in the Croatian part of the Adriatic sea and comparison with wind energy potential. *Energies*, 12(12), 2357. https://doi.org/10.3390/en12122357

[16]   Bento, A. R., Martinho, P., Soares, C. G., 2018. Wave energy assessment for Northern Spain from a 33-year hindcast. *Renewable Energy*, 127, 322-333. https://doi.org/10.1016/j.renene.2018.04.049

[17]   Silva, D., Rusu, E., Soares, C. G., 2013. Evaluation of various technologies for wave energy conversion in the Portuguese nearshore. *Energies*, 6, 1344–1364. https://doi.org/10.3390/en6031344

[18]   Andalusia Energy Agency, 2008. https://www.ideandalucia.es/portal/nodo-agencia-andaluza-de-la-energia/ accessed 21st December 2020.

[19]   Statistics National Institute, 2008. https://www.ine.es/ accessed 21st December 2020.

[20]   Puertos del Estado, 2008. http://www.puertos.es/ accessed 21st December 2020.

[21]   Oceanor, 2009. https://www. Oceanor.com/ accessed 21st January 2021.

[22]   Axystechnologies, 2009. https://axystechnologies.com/ accessed 21st January 2021.

[23]   Soares, C. G., 2008. Hindcast of Dynamic Processes of the Ocean and Coastal Areas of Europe. *Coastal Engineering*, 55(11), 825-826. https://doi.org/10.1016/j.coastaleng.2008.02.007

[24]   Meteorology Statal Agency, 2008. http://www.aemet.es/ accessed 21st December 2020.

[25]   Pastor, J., Liu, Y., 2015. Wave Energy Resource Analysis for Use in Wave Energy Conversion. *Journal of Offshore Mechanics and Arctic Engineering*, 137, 011903-9. https://doi.org/10.1115/1.4028880

[26]   Hagerman, G., 2001. Southern New England Wave Energy Resource Potential. *Building Energy*, Boston, USA.

[27]   Falnes, A., Kurniawan, A., 2015. Fundamental formulae for wave-energy conversion. *Royal Society Open Science*, 2, 1-34. https://doi.org/10.1098/rsos.140305

[28]   Titah-Benbouzid, H., Benbouzid, M., 2015. An Up-to-Date Technologies Review and Evaluation of Wave Energy Converters. *International Review of Electrical Engineering-IREE*, 10(1), 52-61. https://doi.org/10.15866/iree.v10i1.5159

[29]   Soares, C. G., Bhattacharjee, J., Tello, M., Pietra, L., 2012. Review and classification of Wave Energy Converters. Maritime Engineering and Technology. *Taylor & Francis Group*. London, UK, 585-59.

[30]   Falcao, A., 2010. Wave energy utilization: A review of the technologies. Renewable and Sustainable *Energy Reviews*, 14, 899-918. https://doi.org/10.1016/j.rser.2009.11.003

[31]   Diaconu, S., Rusu, E., 2013. Evaluation of various WEC devices in the Romanian near shore. *13th Advances in Environment Technologies, Agriculture, Food and Animal Science*, Brasov, Romani.

[32]   Babarit, A., Hals, J., Muliawan, M., Kurniawan, A., Moan, T., Krokstad, J., 2012. Numerical benchmarking study of a selection of wave energy converters. *Renewable Energy*, 41, 44-63. https://doi.org/10.1016/j.renene.2011.10.002

[33]   Wave Dragon, 2009. www.wavedragon.net accessed 21st January 2021.

[34]   Pelamis, 2009. http://tinyurl.com/pelamis/ accessed 21st January 2021.

[35]   AquaBuoy, 2009. www.inhibitant.com accessed 21st January 2021.

[36]   Archimedes Wave Swing, 2009. http://tinyurl.com/archws1/ accessed 21st January 2021.

[37]   Oceantec, 2008. www. Oceantec.es accessed 21st January 2021.

[38]   Cascajo R., García E., Quiles E., Correcher A., Morant F., 2019. Integration of marine wave energy converters into seaports: A case study in the port of Valencia. *Energies*, 12(5), 787. https://doi.org/10.3390/en12050787

[39]   Rusu E., 2014. Evaluation of the wave energy conversion efficiency in various coastal environments. *Energies*, 7, 4002-40018. https://doi.org/10.3390/en7064002

[40]   Vannuchi V., Cappietti L., 2016. Wave energy assessment and performance estimation of state of the art wave energy converters in Italian hotspots. *Sustainability*, 8 (12), 1300. https://doi.org/10.3390/su8121300

[41]   Rusu E., Soares, C. G., 2012. Wave energy pattern around the Madeira Islands. *Energy*, 45, 771-785. https://doi.org/10.1016/j.energy.2012.07.013

[42]   Bozzi S., Archetti R., Passoni G., 2014. Wave electricity production in Italian offshore: A preliminary investigation. *Renewable Energy*, 62, 407-416. https://doi.org/10.1016/j.renene.2013.07.030